DOI 10.5012/bkcs.2011.32.8.2623

Phase Transition of Octaneselenolate Self-assembled Monolayers on Au(111) Studied by Scanning Tunneling Microscopy

Jungseok Choi, Hungu Kang, Eisuke Ito,† Masahiko Hara,†,‡ and Jaegeun Noh*

*Department of Chemistry and Research Institute for Natural Sciences, Hanyang University, Seoul 133-791, Korea. *E-mail: jgnoh@hanyang.ac.kr*
†Flucto-order Functions Research Team, RIKEN-HYU Collaboration Center, RIKEN, 2-1 Hirosawa, Wako, Saitama 351-0198, Japan
‡Department of Electronic Chemistry, Tokyo Institute of Technology, 4259 Nagatsuta, Midoriku, Yokohama 226-8502, Japan
Received May 22, 2011, Accepted June 20, 2011

We investigated the surface structure and wetting behavior of octaneselenolate self-assembled monolayers (SAMs) on Au(111) formed in a 50 μM ethanol solution according to immersion time, using scanning tunneling microscopy (STM) and an automatic contact angle (CA) goniometer. Closely-packed, well-ordered alkanethiol SAMs would form as the immersion time increased; unexpectedly, however, we observed the structural transition of octaneselenolate SAMs from a molecular row phase with a long-range order to a disordered phase with a high density of vacancy islands (VIs). Molecularly resolved STM imaging revealed that the missing-row ordered phase of the SAMs could be assigned as a $(6 \times \sqrt{3})R30°$ superlattice containing three molecules in the rectangular unit cell. In addition, CA measurements showed that the structural order and defect density of VIs are closely related to the wetting behaviors of octaneselenolate SAMs on gold. In this study, we clearly demonstrate that interactions between the headgroups and gold surfaces play an important role in determining the physical properties and surface structure of SAMs.

Key Words : Octaneselnolate, Self-assembled monolayers, Scanning tunneling microscopy, Phase transition, Contact angle

Introduction

Self-assembled monolayers (SAMs) of organic molecules on solid surfaces have been extensively studied for more than two decades because they can be used as molecular templates for various technological applications, such as corrosion inhibition, biosensors, nanopatterning, and molecular electronics.[1-7] Alkanethiol SAMs with a high degree of structural order on Au(111), in particular, are the most scientifically studied molecular systems because they are ideal systems for understanding self-assembly phenomena of organic molecules. Furthermore, functional monomolecular films can be simply and powerfully generated by modifying the chemical structure of the molecular backbone of alkanethiol SAMs.[1-9] The formation and packing arrangements of SAMs are derived from the complex interplay of intermolecular and headgroup-substrate interactions. Among many analytical techniques, scanning tunneling microscopy (STM) can elucidate a variety of molecular-scale features of alkanethiol SAMs such as packing structure,[1,2,10-13] interface dynamics,[8,9] and the SAM growth mechanism.[14] A previous study demonstrated that alkanethiols SAMs at saturation coverage have a well-ordered $(\sqrt{3} \times \sqrt{3})R30^o$ structure or $c(4 \times 2)$ superlattice with a tilted adsorption geometry of about 30° from the surface normal in an all-trans conformation.

The physical and chemical properties of SAMs can be altered easily by using a different active headgroup to sulfur, such as isocyanide group,[15] selenium,[16] or tellurium.[17] Selenium in particular is expected to be a viable alternative to sulfur, because both elements have similar chemical properties and are neighbors in the VIB column of the periodic table. In contrast to thiol SAMs, however, few studies have investigated the adsorption conditions, molecular orientation, and packing structure of organoselenium SAMs.[18-24] Surface-enhanced Raman spectroscopy (SERS) revealed that selenolate SAMs can be formed *via* cleavage of S-H bond in selenols or cleavage of Se-Se bond in diselenides, which are analogues of thiols or disulfides, upon adsorption.[18-20] A STM study by Disher *et al*. revealed that the adsorption of benzeneselenols (BSe) led to the formation of loosely packed ordered SAMs that could be assigned the $(3\sqrt{3} \times 2\sqrt{3})R30^o$ structure.[21] However, Azzam observed closely-packed BSe SAMs with a $(4\sqrt{3} \times 2\sqrt{3})R30^o$ structure and tip-induced phase transitions of the SAMs from a $(4\sqrt{3} \times 2\sqrt{3})R30^o$ to a $(2\sqrt{3} \times 4)$ structure.[22] It was reported that antracene-2-selenol on Au(111) forms long-range ordered SAMs, whereas antracene-2-thiol forms poorly ordered SAMs, which implies that interactions between the headgroup and gold substrate significantly affect the two-dimensional (2D) order and domain formation of SAMs.[23] Nakano *et al*. demonstrated that decaneselenols on gold surfaces generated stable SAMs, as did alkanethiols.[24] The first molecular-scale STM observations of dodecanselenolate SAMs on Au(111) formed from didodecyl diselenide have a unique packing structure: these SAMs have a closely packed distorted hexagonal packing

structure with a moiré pattern and a missing-row structure with a $(\sqrt{3} \times 3\sqrt{3})R30^{o}$ unit cell, unlike dodecanethiols.[25] Recently, we found that ordered octaneselenolate SAMs on Au(111) derived from dioctyl diselenide were formed at a low concentration ranging from 5 to 50 μM solution, but that disordered SAMs with exceptionally high-density of VIs were formed at higher concentrations ranging from 1 to 5 mM.[26] Contrary to the formation of well-ordered alkanethiol SAMs in a 1 mM solution, ordered selenolate SAMs can be usually formed at a low solution concentration after a short immersion time, usually less than a few hours.[21,22,25-27]

The goal of the present study was to understand why organoselenium shows such different adsorption behaviors and surface structures, unlike thiols. For this purpose, we examined the surface structure of octaneselenolate SAMs on Au(111) formed in a 50 μM ethanol solution of dioctyl diselenide as a function of immersion time using STM. We report the first STM results, which showed an unexpected phase transition of octaneselenolate SAMs from a molecular row phase with a long-range order to a disordered phase with a high density of VIs.

Experimental

Dioctyl diselenide ($CH_3(CH_2)_7Se\text{-}Se(CH_2)_7CH_3$) was synthesized by refluxing Na_2Se_2 with $C_8H_{17}Br$ in methanol for 3 h, according to previously reported methods.[28] The product was purified by chromatography on SiO_2 using hexane as an eluent, and confirmed by NMR analysis. Octanethiol ($CH_3(CH_2)_7SH$) was purchased from Aldrich, and was used without further purification. Au(111) substrates were prepared by thermal evaporation of gold onto freshly cleaved mica sheets in a ultrahigh vacuum condition of 10^{-7}-10^{-8} Torr, as described previously.[29] Octaneselenolate SAMs were prepared by dipping the Au(111) substrates into a freshly prepared 50 μM ethanol solution of dioctyl diselenide at room temperature for 30 sec-24 h. To directly compare the surface structures of thiolate and selenolate SAMs on Au(111) formed from octanethiol and dioctyl diselenide, which have identical alkyl chains, both SAM samples were prepared in 1 mM ethanol solutions of the corresponding compounds at room temperature for 24 h; these are generally considered to be typical preparation conditions to obtain closely-packed ordered alkanethiol SAMs. The SAM samples were then carefully rinsed with pure ethanol and blown dry with nitrogen prior to surface analysis.

STM measurements were carried out in air at room temperature using a NanoScope E instrument (Veeco, Santa Barbara, CA) and a commercially available Pt/Ir tip (80:20). All STM images were corrected in a constant current mode using bias voltages between 0.25 and 0.65 V and tunneling currents between 0.3 to 0.5 nA. Contact angle (CA) measurements were performed using an automatic contact angle goniometer (model: Easydrop DSA20S, KRÜSS, Germany). Water contact angles were measured at RT on the SAM samples using the sessile drop method and are reported as the average value of CAs obtained from five different sample surfaces.

Results and Discussion

Closely-packed ordered alkanethiol SAMs on gold with a $(\sqrt{3} \times \sqrt{3})$ R30° or c(4 × 2) overlayer structure can be prepared by immersing gold substrates in 1 mM solution at room temperature for 24 h. For direct comparison of thiolate and selenolate SAMs, we prepared octanethiolate and octaneselenolate SAMs on Au(111). The SAMs were formed in 1 mM ethanol solutions of the corresponding compounds at room temperature for 24 h. The STM images in Figure 1 show typical surface structures of octanethiolate and octaneselenolate SAMs on Au(111). Surprisingly, the surface structures of the two SAMs were completely different from one other. The adsorption of octanethiol on Au(111) resulted in the formation of closely-packed ordered SAMs with a commensurate c(4 × 2) superlattice with respect to a hexagonal $(\sqrt{3} \times \sqrt{3})$ R30° overlayer (Figure 1(a)). The inset in Figure 1a shows a clearly molecularly resolved STM image of the c(4 × 2) superlattice. We observed three directional ordered domains with a domain angle of 60° or 120° and clear domain boundaries, indicating that the formation of the SAMs was strongly influenced by the three-fold symmetry of the Au(111) lattice. The formation of VIs (dark pits) with a monatomic depth height of 2.4 Å is due to stress release of the gold surface, which usually occurs during the chemisorption of organic molecules, as demonstrated in various thiolate SAMs.[1,2,30] In contrast to octanethiolate SAMs, however, octaneselenolate SAMs formed in 1 mM ethanol solution were composed only of a liquid-like disordered phase without any clear domain boundaries (Figure 1(b)). In addition, selenolate SAMs contained many irregular-shaped VIs, unlike thiolate SAMs. The ratio of the VI area to the total surface area for selenolate SAMs was approximately 18-23%, which is markedly larger than the 8-12% observed for thiolate SAMs. Thus, our results demonstrate that although selenium has the same electron configuration as sulfur, the formation and surface structure of selenolate SAMs are considerably different from those of thiolate SAMs, which implies that interactions between the headgroups and gold surfaces play an important role in determining the final SAM structure. The

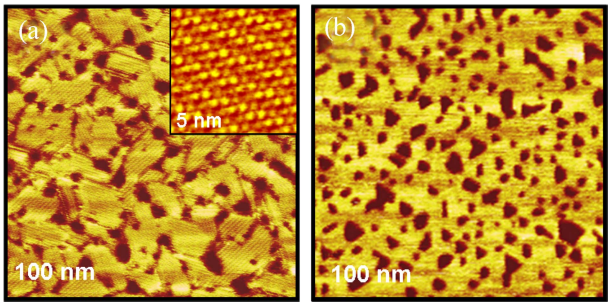

Figure 1. (a) STM images showing surface structures of (a) octanethiolate and (b) octaneselenolate SAMs formed on Au(111) after immersion of the gold substrates in a 1 mM ethanol solution at room temperature for 24 h.

STM results obtained for octaneselenolate SAMs with a disordered phase are different from those reported previously for decaneselenolate or dodecane selenolate SAMs, which have ordered phases.[25] However, it is difficult to compare results directly, because the target materials and SAM preparation conditions were different between studies. Ordered alkane or aromatic selenolate SAMs can usually be obtained at low micromolar solution concentrations after a short immersion time (less than a few hours).[21,22,25-27]

To determine why octaneselenolate SAMs have different surface structures and adsorption behaviors than octanethiolate SAMs, we examined the surface structures of octaneselenolate SAMs on Au(111) formed in a 50 μM ethanol solution as a function of immersion time (0.5 min to 1440 min). We found that a concentration of 50 μM is suitable for monitoring the structural transition of selenolate SAMs from an ordered phase to a disordered phase. However, we observed only disordered phases in a 1 mM solution, irrespective of immersion time, whereas we mainly observed loosely packed ordered phases in a 0.5 μM solution. The STM images of the surface structures of octaneselenolate SAMs on Au(111) show the structural transition from an ordered row structure to a disordered phase surface (Figure 2). After a short immersion of 0.5 min, SAMs with unidirectional, long-range ordered molecular row structures formed over the entire gold surface. Two brightness variations in the molecular rows (A and B regions) were observed, as shown in Figure 2(a). The dark region (A region) contains narrow molecular rows with a row distance of 10 ± 0.3 Å, while the bright region (B region) contains wide molecular rows with a row distance of 20 ± 0.5 Å, which is twice the distance of the dark rows. However, close inspection of the bright rows (C regions) revealed that the wider bright rows were composed of two narrow bright rows with a row distance of 10 ± 0.3 Å. Furthermore, the distance between molecules in a row was 5 ± 0.2 Å, which corresponds to $\sqrt{3}$ of the size of a gold atom. However, we were not able to determine the exact unit cell. The row brightness may be due to differences in the adsorption sites of selenium headgroups or in the adsorption geometry of alkyl tail groups.[5,31] It is unlikely that the observed row structure is a striped phase, where the alkyl chain backbones are oriented parallel to the gold surface, because although the periodicity of the striped phase usually largely depends on the molecular length,[32] the distance between the molecular rows was about 10 ± 0.3 Å, which is smaller than the actual molecular length of octaneselenolates (14.3 Å). At present, it is unclear why octaneselenolate SAMs form such complicated row structures. In addition, in contrast to alkanethiol SAMs, we observed a few, large VIs with lateral dimensions ranging from 8 to 12 nm, and we observed hexagonal-shaped VIs; these findings indicate that the formation of large VIs is closely related to the three-fold symmetry of the Au(111) substrate. The ratio of the VI area to the total surface area for the selenolate SAMs was approximately 6-10%.

As the immersion time was increased to 3 min, new molecular-row ordered domains with different domain orientations and disordered domains appeared, as shown in Figure 2(b). Ordered domains with lateral dimensions of more than 100 nm were still present. The distance between the bright molecular rows was approximately 16.5 ± 1.0 Å. Smaller VIs ranging in size from 1 to 5 nm also emerged, and the number of VIs increased. However, the structural quality of the SAMs did not improve as the immersion time increased. Figure 2(c) shows significant structural changes that were observed in SAMs formed after immersion for 30 min. Ordered domains decreased in size by several nanometers, and clear domain boundaries were observed. The SAMs were composed mainly of ordered phases, but the size of the disordered phases was slightly increased (see Figure 2(b)).

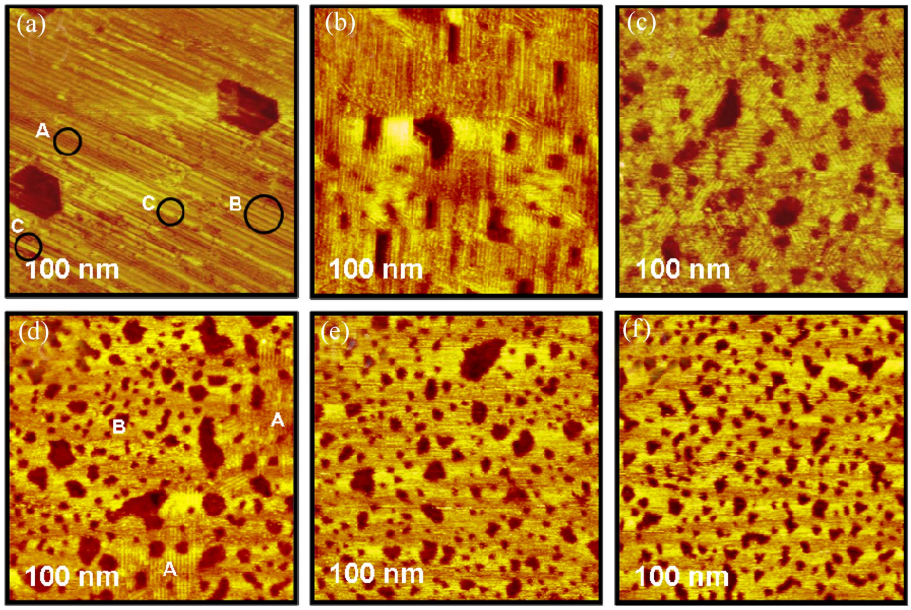

Figure 2. STM images showing phase transition of octaneselenolate SAMs on Au(111) as a function of immersion time: (a) 0.5, (b) 5, (c) 30, (d) 45, (e) 120, and (f) 1440 min in a 50 μM ethanol solution at room temperature.

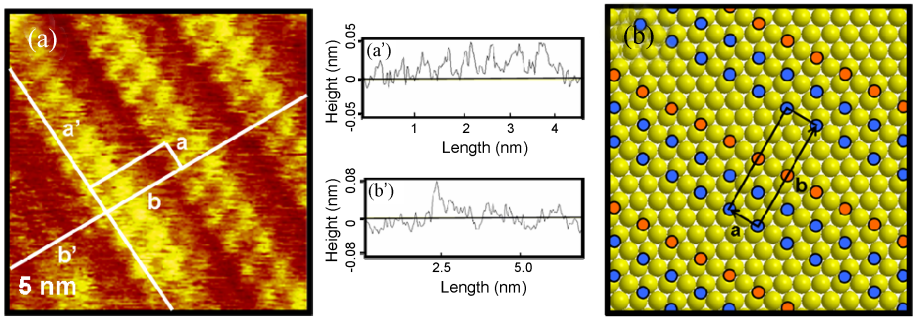

Figure 3. (a) High-resolution STM image showing a missing row phase of octaneselenolate SAMs on Au(111) formed after immersion at room temperature for 45 min. (a' and b') Line profiles along lines a' and b' on the image show the periodicities of the adsorbed molecules. (b) A schematic structural model for octaneselenolate SAMs on Au(111).

The distance between the bright molecular rows was 17.3 ± 0.5 Å, which is nearly similar to the distance observed after immersion for 3 min. Structural details are provided in Figure 3. In addition, the number of small VIs increased. As the immersion time increased to 45 min, two mixed phases containing ordered and disordered phases (A and B regions) were clearly observed (Figure 2(d)). The surface structure of octaneselenolate SAMs on Au(111) changed drastically from an ordered phase to a disordered phase. The disordered phase was the dominant phase. In contrast, after immersion for 120 min (2 h) and 1440 min (24 h), the ordered phases disappeared completely, and disordered phases with abnormally large numbers of VIs formed, as shown in Figures 2e and f. The surface structure of the SAMs and the distribution, density, and number of VIs were quite similar to those observed from an octaneselenolate SAM sample prepared in 1 mM solution for 24 h (Figure 1(b)). Thus, in this study, we demonstrated that a structural transition from an ordered molecular row phase to a disordered phase occurred in octaneselenolate SAMs as the solution immersion time increased. This structural transition of selenolate SAMs is markedly different from that for thiolate SAMs; the phase transition of thiolate SAMs from a low-density striped phase to a closely packed well-ordered phase usually occurs *via* various intermediate phases with increasing immersion time.[14,33,34] The unusual phase transition behavior of selenolate SAMs may be due to the stronger binding affinity of selenium than sulfur.[24,25] This can weaken the interactions between gold atoms in the first gold layers, so that a number of selenolate-gold complexes can easily be released from the gold surface as the surface coverage increases, resulting in the formation of disordered phases with larger fractions of VIs. Another possible reason for the unusual phase transition behavior of SAMs may be the solvent-mediated etching of SAM layers *via* oxidation of selenium headgroups, because the structural transition usually occurred during solution phase deposition. We have found that octaneselenolate SAMs grown from the vapor phase do not grow in the same manner as those grown from solution phase.

The molecularly resolved STM image shown in Figure 3(a) clearly shows the ordered molecular row structure of octaneselenolate SAMs on Au(111) formed after immersion for 45 min. On the basis of the STM observations, we extracted the lattice constants of a rectangular unit cell containing six molecules: a = 5.0 ± 0.2 Å = $\sqrt{2}a_h$ and b = 17.3 ± 0.5 Å = $6a_h$, where a_h = 2.89 Å corresponding to the interatomic distance of the Au(111) lattice. The line profiles along lines a' and b' indicated in Figure 3(a) show the periodicities of the adsorbed molecules. A schematic structural model of octaneselenolate SAMs on Au(111) is provided in Figure 3(b). The molecular packing structure of the SAMs consists of a $(6 \times \sqrt{3})R30^o$ superlattice containing three molecules per rectangular unit cell. The average areal molecular density of the adsorbed molecules was calculated to be 28.83 $Å^2$/molecule, which is comparable to the density of 21.6 $Å^2$/molecule for octanethiolate SAMs with a $(\sqrt{3} \times \sqrt{3})R30°$ structure or a $c(4 \times 2)$ superlattice. The molecular density of octaneselenolate SAMs was 1.3-fold lower than that for octanethiolate SAMs. In addition, the structural model in Figure 3(b) clearly shows that selenolate SAMs have a missing row structure that appeared frequently prior to the formation of closely packed SAMs.[25,29,35] A similar missing row phase has been observed for dodecaneselnolate SAMs with a longer alkyl chain.[25] In the structural model, we also assumed that all selenium atoms in the SAMs occupied bridge sites of the Au(111) lattice. A previous study suggested that either bridge sites or three-fold hollow sites can bind selenium headgroups.[25]

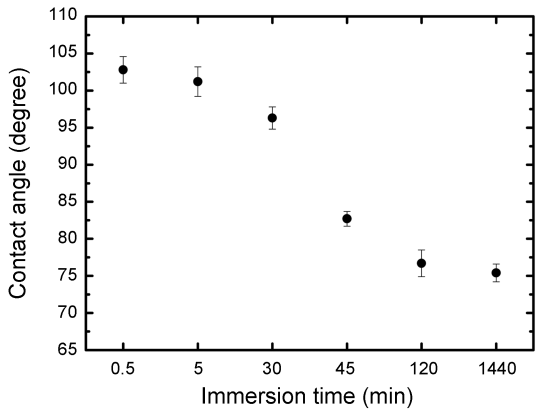

Figure 4. Water static contact angles measured from octaneselenolate SAMs on Au(111) as a function of immersion time: (a) 0.5, (b) 5, (c) 30, (d) 45, (e) 120, and (f) 1440 min in a 50 μM ethanol solution at room temperature.

To understand the relationship between the observed surface structure (Figure 2) and the wetting behavior of octaneselenolate SAMs formed on Au(111) as a function of immersion time, we measured the CAs of the SAMs. Variations in the water contact angle depending on the surface structures of the SAMs grown on Au(111) are shown in Figure 4. We found the following general trend of wetting behavior: SAMs containing order phases (Figs. 2(a)-(c), after immersion for 0.5, 5, and 30 min) had relatively high CAs ranging from 96 to 103°, which implies the formation of a hydrophobic surface due to the presence of a methyl group at the outer SAM surface, whereas SAMs containing disordered phases and an abnormally high density of VIs (Figs. 2(d)-(f), after immersion for 45, 120, and 1440 min) had relatively low CAs ranging from 75 to 83°, which implies the formation of poorly ordered SAMs, as demonstrated by the STM observations. It is clear from our results that structural order and defect density (VIs) strongly affect the wetting behaviors of SAMs on gold.

Conclusions

STM observations revealed that the surface structures of octanethiolate and octaneselenolate SAMs on Au(111) grown in 1 mM ethanol solutions for 24 h differ considerably from each other: octanethiolate SAMs have a well-ordered c(4 × 2) superlattice, whereas octaneselenolate SAMs have a disordered phase with an abnormally high VI density. In contrast to the formation of closely-packed, well-ordered alkanethiol SAMs as the immersion time increased, we found that octaneselenolate SAMs underwent a structural transition from a molecular row phase with an unidirectional, long-range order to a disordered phase with a high density of VIs. Based on high-resolution STM observations, the SAMs with a missing row ordered phase were described as having a $(6 \times \sqrt{3})R30°$ superlattice molecular packing structure with three molecules per rectangular unit cell. The average areal molecular density for the adsorbed molecules was 28.83 $Å^2$/molecule, which is comparable to the average area molecular distance of 21.6 $Å^2$/molecule calculated for octanethiolate SAMs with a c(4 × 2) superlattice. CA measurements also showed that structural order and defect density (VIs) strongly affected the wetting behaviors of octaneselenolate SAMs on gold. Although selenium has the same electron configuration as sulfur, the formation and surface structure of selenolate SAMs are considerably different from those of thiolate SAMs, which implies that interactions between the headgroups and gold surfaces play an important role in determining the physical properties and surface structures of SAMs.

Acknowledgments. This work was supported by a grant from the Korea Research Foundation (KRF) funded by the Korean Government (KRF-2008-313-C00410).

References

1. Love, J. C; Estroff, L. A.; Kriebel, J. F.; Nuzzo, R. G.; Whitesides, G. M. *Chem. Rev.* **2005**, *105*, 1103.
2. Schreiber, F. *J. Phys.: Condens. Matter* **2004**, *16*, R881.
3. Krämer, S.; Fuierer, R. R.; Gorman, C. B. *Chem. Rev.* **2003**, *103*, 4367.
4. Lee, N.-S.; Kim, D.; Kang, H.; Park, D. K.; Han, S. W.; Noh, J. *J. Phys. Chem. C* **2011**, *115*, 5868.
5. Kang, H.; Lee, N.-S.; Ito, E.; Hara, M.; Noh, J. *Langmuir* **2010**, *26*, 2983.
6. Kang, H.; Kim, Y.; Hara, M.; Noh, J. *Ultramicroscopy* **2010**, *110*, 666.
7. Kang, H.; Park, T.; Choi, I.; Lee, Y.; Ito, E.; Hara, M.; Noh, J. *Ultramicroscopy* **2009**, *109*, 1011.
8. Noh, J.; Kato, H. S.; Kawai, M.; Hara, M. *J. Phys. Chem. B* **2006**, *110*, 2793.
9. Noh, J.; Hara, M. *Langmuir* **2002**, *18*, 1953.
10. Li, F.; Tang, L.; Zhou, W.; Guo, Q. *Langmuir* **2010**, *26*, 9484.
11. Kwon, S.; Choi, Y.; Choi, J.; Kang, Y.; Chung, H.; Noh, J. *Ultramicroscopy* **2008**, *108*, 1311.
12. Yang, G.; Liu, G.-Y. *J. Phys. Chem. B* **2003**, *107*, 8746.
13. Kang, H.; Kim, Y.; Park, T.; Park, J. B.; Ito, E.; Hara, M.; Noh, J. *Bull. Korean Chem. Soc*. **2011**, *32*, 1253.
14. Poirier, G. E. *Langmuir* **1999**, *15*, 1167.
15. Murphy, K. L.; Tysoe, W. T.; Bennett, D. W. *Langmuir* **2004**, *20*, 1732.
16. Yoo, H.; Choi, J.; Wang, G.; Kim, T.-W.; Noh, J.; Lee, T. *J. Nanosci. Nanotech*. **2009**, *9*, 7012.
17. Nakamura, T.; Miyamae, T.; Yoshimura, D.; Kobayashi, N.; Nozoye, H.; Matsumoto, M. *Langmuir* **2005**, *21*, 5026.
18. Nakano, K.; Sato, T.; Tazaki, M.; Takagi, M. *Langmuir* **2000**, *16*, 2225.
19. Han, S. W.; Kim, K. *J. Colloid interface Sci*. **2001**, *240*, 492.
20. Han, S. W.; Lee, S. J.; Kim, K. *Langmuir* **2001**, *17*, 6981.
21. Dishner, M. H.; Hemminger, J. C.; Feher, F. J. *Langmuir* **1997**, *13*, 4788.
22. Azzam, W. *Appl. Surf. Sci*. **2010**, *256*, 2299.
23. Bashir, A.; Käfer, D.; Müller, J.; Wöll, C.; Terfort, A.; Witte, G. *Angew. Chem. Int. Ed*. **2008**, *47*, 5250.
24. Nakano, K.; Sato, T.; Tajaki, M.; Tagaki, M. *Langmuir* **2000**, *16*, 2225.
25. Monnel, J. D.; Stapleton, J. J.; Jackiw, J. J.; Dunbar, T.; Reinerth, T.; Dirk, S. M.; Tour, J. M.; Allara, D. L.; Weiss, P. S. *J. Phys. Chem. B* **2004**, *108*, 9834.
26. Choi, J.; Lee, Y.; Kang, H.; Han, J. W.; Noh, J. *Bull. Korean Chem. Soc*. **2008**, *29*, 1229.
27. Shaporenko, A.; Ulman, A.; Terfort, A.; Zharnikov, M. *J. Phys. Chem. B* **2005**, *109*, 3898.
28. Gladysz, J. A.; Hornby, J. L.; Garbe, J. E. *J. Org. Chem*. **1978**, *43*, 1204.
29. Choi, Y.; Jeong, Y.; Chung, H.; Ito, E.; Hara, M.; Noh, J. *Langmuir* **2008**, *24*, 91.
30. Poirier, G. E. *Chem. Rev.* **1997**, *97*, 1117.
31. Riposan, A.; Liu, G.-Y. *J. Phys. Chem. B* **2006**, *110*, 23926.
32. Camillone, N.; Leung, T. Y. B.; Schwartz, P.; Eisenberger, P.; Scoles, G. *Langmuir* **1996**, *12*, 2737.
33. Noh, J.; Hara, M. *RIKEN Review* **2001**, *38*, 49.
34. Vericat, C.; Vela, M. E.; Benitez, G.; Carro, P.; Salvarezza, R. C. *Chem. Soc. Rev.* **2010**, *39*, 1805.
35. Noh, J. Hara, M. *Langmuir* **2001**, *17*, 7280.